

# Tensile Fracture Behavior in Wrought Magnesium Alloy Fabricated by Multi-Directional Forging Technique

Akihiro Takahashi<sup>1</sup>, Hiromi Miura<sup>2</sup>, Masakazu Kobayashi<sup>3</sup>

<sup>1</sup>Department of Mechanical Engineering

National Institute of Technology (KOSEN), Miyakonojo College, Miyakonojo, Miyazaki 885-8567, Japan

<sup>2,3</sup>Department of Mechanical Engineering, Toyohashi University of Technology, Toyohashi, Aichi 441-8580, Japan

**Abstract-** Hot-extruded AZ31 magnesium alloy was treated by multi-directional forging (MDF) technique up to a maximum cumulative strain of  $\epsilon = 2.4$ . The MDF temperature was decreased pass by pass from 623 K to 493 K. The average grain size decreased as cumulative strain was increased due to dynamic recrystallization (DRX). It was confirmed that MDF technique was effective to make finer and uniform equiaxed microstructure of AZ31Mg alloy. In particular, a drastically change of the evolved microstructure and stress-strain response were obviously recognized at the early pass of MDF stage. The relationship between micro-Vickers hardness, HV and grain size, D can be approximated by a Hall-Petch type equation,  $HV = H_0 + kD^{-1/2}$ , here,  $H_0 = 451$  MPa and  $k = 0.28$  MPa/m<sup>1/2</sup> in this study. As results of experimental observations, it was summarized that main fracture behavior of hot-extruded AZ31Mg alloy was large slip deformation and consequently shear rupture in grains and grain boundaries, on the other hand, that of MDFed AZ31Mg alloy was coalescence of small voids taken place with uniform distribution in the evolved microstructure.

**Keywords** –magnesium alloy, multi-directional forging, microstructure, tensile characterization, fracture behavior

## I. INTRODUCTION

Light-weight materials have potential for weight saving of products for improving fuel consumption and emissions in transportation and logistics systems. CO<sub>2</sub> emissions of new passenger cars registered in Europe are monitored in order to meet the objectives of Regulation EC 443/2009. According to the standards, this calls for an average CO<sub>2</sub> emission of 130 g/km for new passenger cars registered in Europe to be met by vehicle measures in 2015, and this requests to decrease up to 95 g/km in 2020.[1]. Therefore, there is a growing trend to substitute these nonferrous materials for conventional steel and ferrous cast iron especially in automobile parts. For this purpose, the mechanical properties of the nonferrous materials need to approach that of ferrous materials such as ductility, formability, strength and so on. Magnesium (Mg) alloys have the higher specific modulus and strength among other structural metallic materials, and can be beneficial to weight reduction of transportation mechanics. However, it is well known that anisotropic behavior, tensile ductility and formability of Mg alloy sheet at room temperature are limited due to its hexagonal crystal structure [2]. There have been various researches aiming at improving the ductility and strength of Mg alloys through grain refinement using various methods of severe plastic deformation (SPD) processes, e.g., Multi-Directional Forging (MDF) [3], Equal Channel Angular Press (ECAP) [4] and High Pressure Torsion (HPT) [5]. Xing et al [6] presented that the ultrafine grained (UFGed) Mg-3Al-1Zn alloy produced by MDF technique, where its grain size is approximately 300 nm with cumulative strain,  $\epsilon$  of 5, reaches tensile ductility (20 %) and strength (530 MPa) at room temperature. Miura et al [7] reported that UFGed Mg-6Al-1Zn alloy up to  $\epsilon = 4.0$  processed by MDF shows a superior balance of tensile ductility of over 20 % and tensile strength of 440 MPa. Recently, Miura et al [8] applied MDFing to Mg-8Al-0Zn alloy with  $\epsilon = 1.5$  and achieved tensile ductility of about 22 % and tensile strength of 445 MPa at strain rate of  $3.0 \times 10^{-2}$  s<sup>-1</sup>. On the other hand, because of lower ductility of Mg alloys at room temperature, MDF is always carried out at warm temperatures. Thermal atmosphere causes the occurrence of dynamic recrystallization (DRX) phenomena in microstructure, which will be suppression of crack initiation during MDF as a result. References by Miura [6-8] are sufficient reports on grain refinement and enhancement of tensile ductility and strength of wrought Mg alloys applied MDF technique. For increasing a predominance on MDF technique from viewpoint of material development, it is necessary to grasp deformation and fracture morphology. Therefore, the purpose of this work is to investigate fundamentally tensile properties and its fracture behavior at room temperature and evolved microstructure of MDFed AZ31 magnesium alloy.

## II. EXPERIMENTAL PROCEDURE

The material used in the present study is a commercial hot-extruded AZ31 Mg alloy as-received. The chemical composition of the alloy is shown in Table 1. Artificial aging treatment for the alloy was not conducted in particular. The alloy was cut into rectangular shaped sample with initial dimensions of  $a = 14$  mm,  $b = 31$  mm and  $c = 21$  mm

(i.e., aspect ratio,  $a : b : c = 1.00 : 2.22 : 1.49$ ), where an axis of  $b$  dimension is equal to extrusion direction of the alloy. MDF was carried out at a constant true strain rate of  $3 \times 10^{-3} \text{ s}^{-1}$  by using an Amstar-type universal testing machine. The sample was deformed by MDF with changing the loading axis at an angle of  $90^\circ$  from pass to pass as schematically shown in Fig. 1. A pass strain  $\Delta \epsilon$  is employed at a constant (i.e.  $\Delta \epsilon = 0.8$ ). The aspect ratio of the sample is geometrically unchanged during each pass. During MDF, forging temperature was gradually decreased pass by pass from 623 K to 493 K as represented in Fig. 2. The first MDFing axis was parallel to the extruded axis. The samples were MDFed to cumulative strain of  $\epsilon = 2.4$  at maximum, i.e., 3 passes of MDFing. Lubricant (molybdenum disulfide) was used on the forging die surface to prevent bulging and galling of the samples. The sample could be uniformly forged without any cracking even at temperature of 493 K. Tensile testing specimen was cut from the hot-extruded and MDFed samples by electric discharge machine. Five tensile specimens were prepared at each MDF pass. The longitudinal direction of tensile specimen of hot-extruded was correspond to an extrusion direction (E.D.) and that of MDFed also was correspond to direction perpendicular to the last compressive forging axis (F.A.) (see Fig. 3). Fig. 4 shows configuration and dimensions of the tensile specimen in the present study. Hardness test was carried out on the planes parallel to the forging axis (F.A.). Hardness was measured using a micro-Vickers hardness testing machine with an indentation load of 7.35 N for 15 s. The simple average of 10 data was used as the measured hardness value. Microstructure of the hot-extruded and MDFed samples were observed through optical microscope (OM) on three-axial planes. The samples were metallurgically polished and etched in a solution containing 10 ml acetic acid, 12.5g picric acid, 20 ml distilled water and 200 ml ethanol (95%). Average grain size was measured by the linear line-intercept method [9] from OM image. Tensile test using universal testing machine was carried out at room temperature with initial strain rate of  $2.8 \times 10^{-3} \text{ s}^{-1}$ . A strain gage (Kyowa Dengyo Corp., KFEM-1-120) was attempted on plane of a tensile specimen for measuring elastic modulus and 0.2 % proof stress. Scanning electron microscope (SEM) was used to observe fracture surface after tensile test of each specimen.

Table - 1 Chemical composition of the commercial AZ31 Mg alloy used in present study (mass %)

Al	Zn	Mn	Fe	Si	Cu	Ni	Ca	other	Mg
2.5-3.5	0.5-1.5	$\geq 0.2$	$\leq 0.03$	$\leq 0.01$	$\leq 0.01$	$\leq 0.005$	$\leq 0.04$	$\leq 0.03$	Bal.

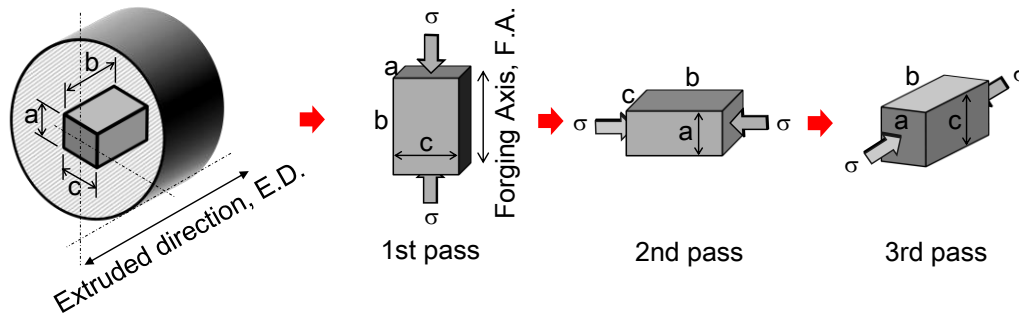


Figure 1. Schematic illustration of the multi-directional forging technique when one pass strain,  $\Delta \epsilon = 0.8$  is employed. Numbers indicate the aspect ratio of  $a : b : c = 1.00 : 2.22 : 1.49$ . Forging axis is tilted to  $90^\circ$  at each pass.

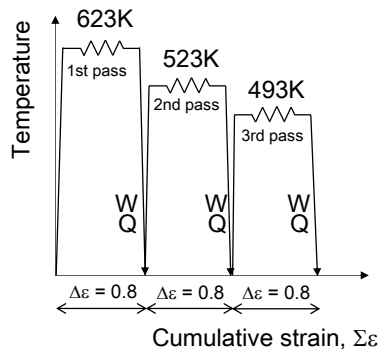


Figure 2. Thermo-mechanical profile of MDF technique in present study

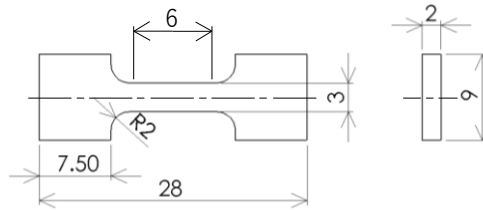


Figure3. Showing illustration of the configuration and dimensions of the tensile specimen in present study

### III. RESULTS AND DISCUSSIONS

#### 3.1. Microstructural evolution –

Fig. 4 shows result of evolved microstructural at all samples. Arrows in figure indicate the extruded direction of (a) and forged direction of (b) to (d), respectively. As a result, the average grain size,  $D$  determined by line-intercept method decreases gradually with increasing cumulative strain from  $16.7 \mu\text{m}$  to  $3.5 \mu\text{m}$  due to DRX. Coarse grains are still observed in MDFed sample of 1st pass. However coarse grain disappears gradually with increasing cumulative strain. In that of 3rd pass, equiaxed crystals having an average grain size of  $3.5 \mu\text{m}$  are obtained, the coarse grain hardly observed as shown in Fig. 4, (d). It is confirmed that MDF process is effective to make finer and uniform microstructure of AZ31Mg alloy.

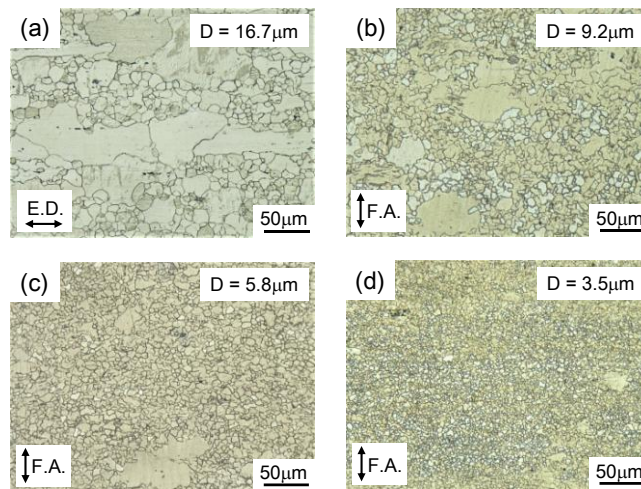


Figure4. Microstructures of the AZ31 alloy evolved during MDF

#### 3.2 Micro-Vickers hardness–

Micro-Vickers hardness change during MDF was investigated and the findings are summarized in Table 2. It can be seen in Table 2 that the hardness increases proportionally with increasing cumulative strain. Additionally, we cannot deny that standard deviation decreases as cumulative strain increases. Equiaxed crystal grains during MDF has uniformly brought about low standard deviation in hardness value at each cumulative strain.

It is known that relationship between hardness, HV and the average grain size,  $D$  (m) evolved during MDF is given by the following Hall-Petch type eq. (1) [6],

$$HV = H_0 + kD^{-1/2} \quad (1)$$

where, unit of HV was converted to MPa. In present study,  $H_0 = 451 \text{ MPa}$ , and  $k = 0.28 \text{ MPa}/\text{m}^{-1/2}$ . According to Xing et al. [6],  $H_0 = 510 \text{ MPa}$  and  $k = 0.22 \text{ MPa}/\text{m}^{-1/2}$  in MDFed AZ31Mg alloy was reported. Yuan et al. [10] and Koike et al. [11] have reported that the relationship between yield stress,  $\sigma_y$  and grain size  $D$  for several Mg alloys could be given by following Hall-Petch eq. (2),

$$\sigma_y = \sigma_0 + kD^{1/2} \quad (2)$$

where,  $\sigma_0$  is  $103 \text{ MPa}$  and  $k$  is  $0.24 \text{ MPa}/\text{m}^{-1/2}$  [10] and  $\sigma_0$  is  $90\text{--}210 \text{ MPa}$  and  $k$  is  $0.17 \text{ MPa}/\text{m}^{-1/2}$  [11]. Empirically, it is known that the formula,  $\sigma_y = 1/3HV$  holds. Using the formula to references [10] and [11], it becomes  $H_0 = 309 \text{ MPa}$  and  $k = 0.24 \text{ MPa}/\text{m}^{-1/2}$  (Yuan et al.) and  $H_0 = 270\text{--}630 \text{ MPa}$  and  $k = 0.17 \text{ MPa}/\text{m}^{-1/2}$  (Koike et al.). The data of  $H_0$  and  $k$  in present study approximately similar to results of Xing et al. [6], Yuan et al. [10] and Koike et al. [11].

Table - 2 Result of the micro-Vickers hardness of MDFed AZ31Mg samples in present study

Sample	Cumulative strain, $\Sigma \epsilon$	Micro- Vickers Hardness, HV
Hot-extruded	0	53±3.2
1st pass	0.8	55±1.4
2nd pass	1.6	59±1.0
3rd pass	2.4	61±1.0

### 3.3 Stress-strain curve in MDFed specimen–

Fig. 5 shows nominal stress-strain curves at each hot-extruded and various MDFed tensile specimen tested at room temperature. The curve of the hot-extruded forms elastic-perfectly plastic body response, which has 0.2 % proof stress,  $\sigma_{0.2}$  of 206 MPa, tensile strength  $\sigma_B$  of 258 MPa and fracture strain,  $\epsilon_f$  of 0.258. On the other hand, the curve of the MDFed specimen of 1st pass forms elastoplastic response owing to work-hardening deformation, which has  $\sigma_{0.2}$  of 117 MPa,  $\sigma_B$  of 254 MPa and  $\epsilon_f$  of 0.344. Symbol, (a) and (b) show  $\sigma_{0.2}$  point of hot-extruded and 1st pass MDF specimen, respectively. A drastically change of the stress-strain response was confirmed after the early pass of MDF stage. These result suggested that a certain crystalline texture of hot-extruded sample is scrapped by one MDF process. As above mentioned, the MDF process with decreasing temperature during forging is employed as explained in Figs. 1 and 2. Because of that, finer crystalline grains with low dislocation density due to DRX form at the early MDF stage. As a result, lower  $\sigma_{0.2}$  and higher  $\epsilon_f$  of 1st pass specimen occurred as compared with those of hot-extruded. All values of the mechanical properties are listed in Table 3.

### 3.4 Fracture surface observation–

Fractography by SEM for the hot-extruded, (a), MDFed of 1st pass specimen, (b) and that of 3rd pass specimen, (c) as shown in Fig. 6 was carried out. The observation direction is corresponding to tensile direction in Fig. 6. SEM micrograph in Fig. 6, (a) shows a combination of small dimples and shear cracks having metallurgical orientation similar to quasi-cleavage crack indicated arrows in the figure. Tear ridges may be perceived at the edges of the dimples and shear cracks. On the other hand, the fracture surface of the 1st pass specimen is almost bare of the shear crack as shown in Fig. 6, (b). In Fig. 6, (c), many holes indicated arrows and small equiaxed dimples which are formed in alignment with the tensile direction are observed. Fig. 6, (b) and (c) are typical ductile fracture surface and its result is an agreement with tensile experimental findings: Fig. 5 and Table 3, where the fracture strain of the MDFed specimen is higher than that of the hot-extruded specimen. By the way, in all micrographs, intermetallic particles such as inclusions, dispersoids and precipitations are not perceived. In general, the dimple is progressed by the process of void nucleation at particles, growth and coalescence [12]. The small void nucleation site originates from the intermetallic particle (i.e. second phase particles). However, the particles are not observed on microstructures in Fig. 4, because AZ31Mg alloy is a kind of solid solution type. Thus, it should be noted that it is necessary to consider another dimple formation mechanism without the particles.

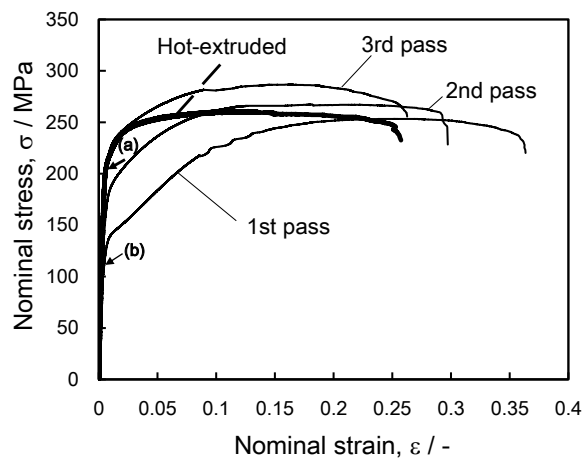


Figure 5. Stress-strain curves tested at room temperature in present study

Table - 3 Mechanical properties obtained by tensile tests of the hot-extruded and MDFed AZ31Mg specimens

Sample	Cumulative strain, $\Sigma\varepsilon$	Elastic modulus, E, GPa	0.2% Proof stress, $\sigma_{0.2}$ , MPa	Tensile strength, $\sigma_B$ , MPa	Fracture strain, $\varepsilon_f$ , (-)
Hot-extruded	0	45	206±5.0	258±10	0.258±0.002
1st pass	0.8	42	117±10	254±3.0	0.344±0.018
2nd pass	1.6	43	159±6.0	268±3.0	0.314±0.012
3rd pass	2.4	45	194±10	285±5.0	0.289±0.019

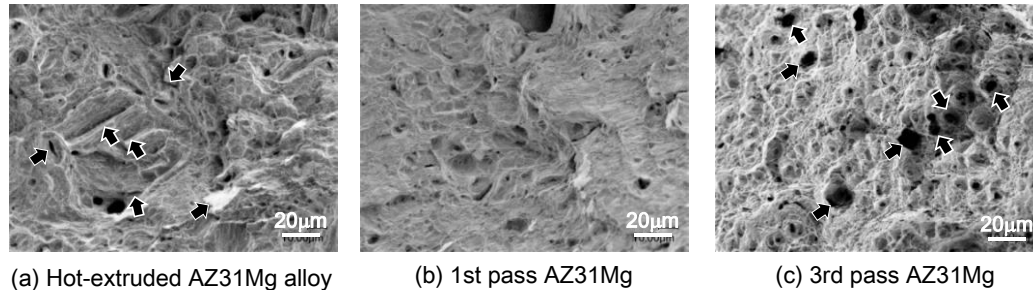


Figure 6. SEM micrographs of the fracture surface of the hot-extruded, (a), MDFed of 1st pass specimen, (b) and that of 3rd pass specimen, (c)

In Fig. 7, microstructures: (a) macroscopic and (b) high magnification near fracture surface, viewed from a side plane of the hot-extruded tensile specimen observed after tensile test. Coarse shear cracks are observed at near fracture surface and at corner of the specimen. It is quite possible that coalescence of shear cracks forms final crack path as shown in Fig. 7, (a). Fig. 7, (b) shows magnification view of the microstructure near fracture surface in Fig. 7, (a). Lots of slip bands and profuse twinning can be seen in many grains. Dense slip bands are made along to a certain orientations based on hot-extruded texture. The orientations of the bands in the grain interior are different depending on each grain. Additionally, shear cracks and small holes indicated symbol “S” and “H” respectively are evidently also observed. Shear cracks took place along to slip bands and grain boundaries at large strain regions. Furthermore, small holes arrowed “H” in the figure initiate triple points on the grain boundary and equiaxed fine grains. It is found that main fracture behavior at hot-extruded specimen is inter- and transgranular shear slip deformation and rupture.

In Fig. 8, microstructures: (a) macroscopic and (b) high magnification near fracture surface, viewed from a side plane of the MDFed 3rd pass specimen observed after tensile test. In Fig. 8, (a), development at necking deformation of the 3rd pass tensile specimen strongly progresses as compared with that of the hot-extruded. Moreover, many small holes arrowed “H” in the figure initiate at equiaxed fine grains with uniform distribution in the microstructure. Observed holes are circular shape, consequently, it occurs lower stress concentration in comparison to a shear shape crack. Furthermore, the multiaxial stress state in the internal necking between holes urges shear stress component to be lower. It is found that main fracture behavior at MDFed specimen is coalescence of small holes.

These findings were shown to be in relative agreement with fracture behavior as represented in Fig. 6 obtained through experimental fracture surface observation.

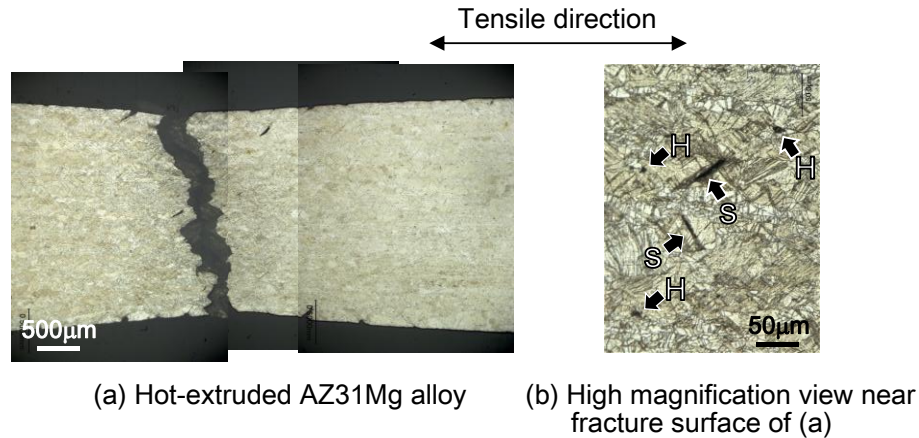


Figure7. Microstructure of the macroscopic photograph, (a) and high magnification view near fracture surface, (b) of the hot-extruded specimen

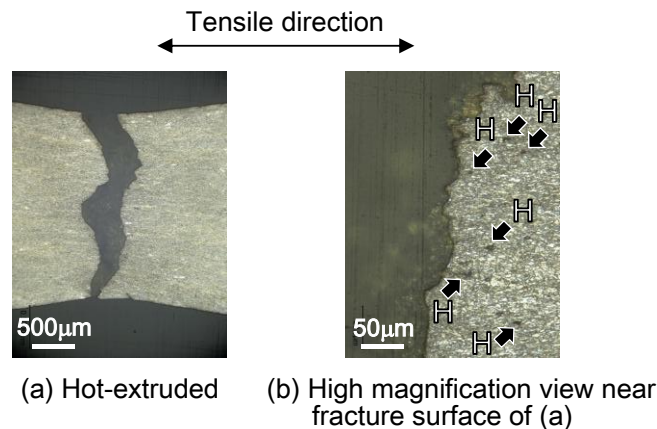


Figure8. Microstructure of the macroscopic photograph, (a) and high magnification view near fracture surface, (b) of the MD Fed 3rd pass specimen

#### IV. CONCLUSION

AZ31Mg alloy was multi-directional forged (MD Fed) at decreasing temperature condition. Tensile test, observation of microstructure and fracture surface at hot-extruded and MD Fed sample up to 3rd passes (i.e. cumulative strain of  $\square \square \square = 2.4$ ). The findings are summarize as follows:

1. The average grain size decreased as cumulative strain was increase due to dynamic recrystallization. It was confirmed that MD Fed technique was effective to make finer and uniform microstructure of AZ31Mg alloy.
2. The relationship between micro-Vickers hardness, HV and grain size, D can be approximated by a Hall-Petch type equation,  $HV = H_0 + kD^{-1/2}$ , here,  $H_0 = 451 \text{ MPa}$  and  $k = 0.28 \text{ MPa}\cdot\text{m}^{-1/2}$ . These are corresponding to results by another researchers.
3. As results of experimental observations, it was summarized that main fracture behavior of hot-extruded AZ31Mg alloy was large slip deformation and consequently shear rupture in grains and grain boundaries, on the other hand, that of MD Fed AZ31Mg alloy was coalescence of small holes taken place with uniform distribution in the evolved microstructure.

#### V. ACKNOWLEDGMENT

This study was supported by Toyohashi University of Technology (Research No. 2105) and the AMADA foundation (AF-2016021). The authors also appreciate the financial assistance of the Light Metal Educational Foundation, Japan.

## VI. REFERENCES

- [1] G.Mellios, S. Hausberger, M.Keller, C. Samarasand L. Ntziachristos,“Parameterisation of Fuel Consumption and CO2 Emissions of Passenger Cars and Light Commercial Vehicle for Modelling Purposes”, JRC Scientific and Technical Reports,2-6 , 2011
- [2] S. Yi, “Mechanical Anisotropy and Deep Drawing Behaviour of AZ31 and ZE10 Magnesium Alloy Sheets”, Acta Mater., vol.58, 592-605, 2010
- [3] J. Xing, X. Yang, H. Miura and T. Sakai“Mechanical Properties of Magnesium Ally AZ31 after Severe Plastic Deformation”Mater. Trans. J, vol. 49, 69-75, 2008
- [4] H. Watanabe, A. Takara, H. Somekawa, T. Mukaiand K. Higashi,“Effect of Texture on Tensile Properties at Elevated Temperatures in an AZ31 Magnesium Alloy”Scr. Mater., vol. 52, 449-454, 2005
- [5] M. Kai, Z. Horita, T. G. Langdon,“Development Grain Refinement and Superplasticity in a Magnesium Alloy Processed by High-Pressure Torsion” Mater. Sci. Eng. A., vol. 488,117-124, 2008
- [6] J. Xing, X. Yang, H. Miura and T. Sakai“Ultra-Fine Grain Development in an AZ31 Magnesium Alloy during Multi-Directional Forging under Decreasing Temperature Conditions”Mater. Trans. JIM., vol. 46, 1646-1650, 2005
- [7] H. Miura, G. Yu, X. Yang and T. Sakai “Microstructure and Mechanical Properties of AZ61 Mg Alloy Prepared by Multi Directional Forging ”Trans. Nonferrous Metals Sci. China, vol. 20, 1294-1298, 2010
- [8] H. Miura, M. Kobayashi and T. Benjanarasuth“Effects of Strain Rate during Multi-Directional Forging on Grain Refinement and Mechanical Properties of AZ80Mg Alloy ”Mater. Trans., vol. 57, 1418-1423, 2016
- [9] H. Abrams, “Practical Applications of Quantitative Metallography ”ASTM STP 504, 138-182, 1972
- [10] W. Yuan, S. K. Panigrahi, J. Q. Su and R. S. Mishra, “Influence of Grain Size and Texture on Hall-Petch Relationship for a Magnesium Alloy”Scripta. Meter., vol. 65, 994-997, 2011
- [11] J. Koike,“Strength and Ductility of Mg Alloys ”Proc. Of the 4th Pac. Rim Int. Conf. of Advanced Mater. and Processing, 1179-1182, 2001
- [12] J. F. Knott, “Fundamentals of Fracture Mechanics ”Butterworths, 1973